A Study on Performance Characterization Considering Six-Degree-of-Freedom Vibration Stress and Aging Stress for Electric Vehicle Battery Under Driving Conditions

Li, Wenhua; Jiao, Zhipeng; Xiao, Qian; Meng, Jinhao; Mu, Yunfei; Jia, Hongjie; Teodorescu, Remus; Blaabjerg, Frede

Published in:
IEEE Access

DOI (link to publication from Publisher):
10.1109/ACCESS.2019.2935380

Publication date:
2019

Document Version
Publisher's PDF, also known as Version of record

IEEE Access
Multidisciplinary | Rapid Review | Open Access Journal

Received July 27, 2019, accepted August 11, 2019, date of publication August 14, 2019, date of current version August 26, 2019.

Digital Object Identifier 10.1109/ACCESS.2019.2935380

A Study on Performance Characterization Considering Six-Degree-of-Freedom Vibration Stress and Aging Stress for Electric Vehicle Battery Under Driving Conditions

WENHUA LI[1,2], (Member, IEEE), ZHIPENG JIAO[1], QIAN XIAO[3,4], JINHAO MENG[5], (Student Member, IEEE), YUNFEI MU[3], (Member, IEEE), HONGJIE JIA[3], (Senior Member, IEEE), REMUS TEODORESCU[4], (Fellow, IEEE), AND FREDE BLAABJERG[4], (Fellow, IEEE)

[1]State Key of Laboratory of Reliability and Intelligence of Electrical Equipment, Hebei University of Technology, Tianjin 300130, China
[2]Key Laboratory of Electromagnetic Field and Electrical Apparatus Reliability of Hebei Province, Hebei University of Technology, Tianjin 300130, China
[3]Key Laboratory of Smart Gird of Ministry of Education, Tianjin University, Tianjin 300072, China
[4]Department of Energy Technology, Aalborg University, 9220 Aalborg, Denmark
[5]School of Automation, Northwestern Polytechnical University, Xi'an 710072, China

Corresponding author: Qian Xiao (xiaoqian@tju.edu.cn)

This work was supported in part by the Youth Fund Project of Hebei Education Department under Grant QN2017316, in part by the National Key Research and Development Program of China under Grant 2017YFB0903300, in part by the project of the National Natural Science Foundation of China under Grant 51625702 and Grant 51807135, and in part by the Joint Fund Project of the National Natural Science Foundation-State Grid Corporation under Grant U1766210.

ABSTRACT The battery degradation tests under various stress are critical to understand the relationship between the battery lifespan and the external factors. This paper establishes a battery test bench, which can provide not only the 6-six degree of freedom (DOF) vibration stress but also the charge-discharge stress. By conducting lithium-ion batteries under 6-DOF vibration stress and other reference experiments, the electrochemical impedance spectroscopy (EIS), internal resistances, thermal measurement, open circuit voltage (OCV) recovery and capacity of the cells are compared to determine the impact of the 6-DOF vibration stress on the cells. The experimental results show that the vibration stress increases the ohmic resistance, and also causes a higher heat release. In addition, the cells under vibration stress exhibit a higher capacity fade and a lower OCV recovery rate, while the internal impedance is also changed with vibration stress. In order to quantize the effect of the vibration stress on battery degradation, the analysis of variance (ANOVA) is calculated. The conclusion is that the vibration stress has little impact on the cell polarization resistance, while it significantly affects the ohmic resistance, OCV recovery, thermal measurement, and capacity of cells, respectively.

INDEX TERMS Electric vehicle (EV), lithium-ion battery, six-degree-of-freedom (6-DOF) vibration stress, performance test, analysis of variance (ANOVA).

I. INTRODUCTION

With the popularization of lithium-ion batteries in hybrid electric vehicles and electric vehicles (HEVs, EVs), further research of the cells' performance is necessary to avoid battery failure during driving [1]–[3].

However, faults of lithium-ion batteries lead to not only serious inconvenience and enormous maintenance cost, but also the risk of catastrophic consequences, for example battery swelling due to overheating or short circuit [4]–[7].

In order to investigate the performance or characterization of battery under vibration stress, several scholars have done similar research work. In [8], a new vibration test methodology was proposed to understand the attribution of 6-DOF vibration stress to the electromechanical performance of nickel cobalt aluminium oxide (NCA) 18650 cells. And the electrical and mechanical degradation post were quantified under vibration stress. With porous graphene

The associate editor coordinating the review of this article and approving it for publication was Xiaosong Hu.

oxide-nickel (pGO-Ni) electrode and ionic solution, a novel method converting vibration energy to EV was presented [9]. In [10], test profiles were used to provide batteries with stress and capacity measurement, impedance spectroscopy, micro-X-ray computed tomography and post mortem analyses were utilized to reveal how lithium-ion batteries are affected by vibration and shock. Considering electrodynamic vibration system model and vibration test, the vulnerable part for fatigue failure of a 12 V/75 Ah valve regulated lead-acid battery was uncovered under scanning electron microscope (SEM) [11]. The contributions of [12] are investigating how proton exchange membrane fuel cells (PEMFCs) are affected under shock and vibration, and comparing effects of four kinds of vibration: shock, harmonic, random, and real-world vibration. Due to prestress and battery parameters difference, a new numerical methodology was proposed and the Monte Carlo simulations are used to test the effects of cell-to-cell variations [13]. Considering intercalation and multiple swelling sources about driving conditions, a 1-D phenomenological force model of lithium-ion cell was developed, which contributes to investigating dynamic states of cells and packs [14]. The phenomenon that external vibrations lead to the internal destruction of the cells was found. In addition, the effect of vibration on the parameters and mechanism of cells was investigated [15]. And some articles concentrated on charge-discharge protocols to reveal how batteries perform under different rates [16]–[18].

However, it is not enough for testing battery that only vibration stress or aging stress was taken into consideration. Combined the charge-discharge process with the vibration stress, the performance and degradation of lithium-ion batteries under single DOF vibration stress and aging stress were investigated, and the prognosis for residual useful life of cells was developed [19]–[20].

Nevertheless, prior researches on the above mentioned factors (i.e. only single DOF vibration stress or aging stress was applied to batteries) on performance and the characteristics of the LIBs are limited in amount and scope. Especially, the impact of 6-DOF vibration stress on the battery is often neglected. Hence, in this paper, 6-DOF vibration stress was applied to batteries and EV test profile was applied to the lithium-ion cells for aging stress, both of which are to simulate the real-world driving environment.

In our view, the main contributions of this paper as follows:

1) The experimental bench under 6-DOF vibration stress and aging stress was established, which not only provides 6-DOF vibration stress but also conducts the aging test.

2) By conducting four experimental profiles, the characteristics of the cells under different tests, including EIS, internal resistances, thermal measurement, OCV recovery and capacity, were investigated. In addition, these characteristics were compared to determine the impact of 6-DOF vibration stress and aging stress on the cells.

3) Based on ANOVA, the impact of the vibration stress with aging on cells was proved statistically.

The rest of this paper is organized as follows. In Section 2, the experimental setup and performance tests are introduced; Section 3 exhibits the test results from the aspects of initial characteristics, internal resistances, internal impedance, thermography and temperature measurement, OCV recovery and capacity degradation; According to analysis of variance (ANOVA), these characteristics can be compared statistically to determine the impact of the vibration stress with aging on cells in Section 4; The conclusion and prospects are in Section 5.

II. EXPERIMENTS

The battery testing instrument Arbin LBT-60V100A, internal impedance testing instrument Solartorn Analytical EnergyLab XM, thermal recorder TOPRIE TP900 (Shenzhen, China), thermography camera FLIR T420 and 6-DOF vibration stress environment platform RUISUN (Jiangsu, China) were used to construct this experimental bench as Figure 1. The 15 cylindrical lithium-ion cells LR16850EH LISHEN (Tianjin, China) were chosen as the test samples in this experiment.

The function of these parts in this experimental system is as follows:

(1) Arbin LBT-60V100A: conduct charging-discharging protocol.

(2) Solartorn Analytical EnergyLab XM: test the internal impedance.

(3) TOPRIE TP900 (Shenzhen, China): record thermal measurement.

(4) FLIR T420: reveal thermography.

(5) RUISUN (Jiangsu, China): provide 6-DOF (roll angle φ, pitch angle θ, yaw angle ω, ΔX, ΔY and ΔZ) vibration stress.

(6) LR16850EH LISHEN (Tianjin, China): as experimental object and the nominal specifications is as Table 1.

TABLE 1. Nominal specifications of the selected cells.

Item	Specification
Cathode material	$LiFePO_4$
Anode material	Graphite
Nominal capacity	1530 mAh
Maximum charge current	1.0 C
Charge cut-off voltage	3.65 V
Maximum discharge current	2.0 C
Discharge cut-off voltage	2.0 V
Operating temperature	Charge: 0~ +45 ℃ Discharge: -20~ +60 ℃

In order to demonstrate the merits of this experimental bench, characteristics contrast of experimental bench between this paper and some others is shown in Table 2.

III. EXPERIMENTAL PROFILE

A. INTERNAL CHARATCTERISTICS TEST

Before the experiments, it is necessary for those batteries to be conducted three cycles to activate themselves. In order

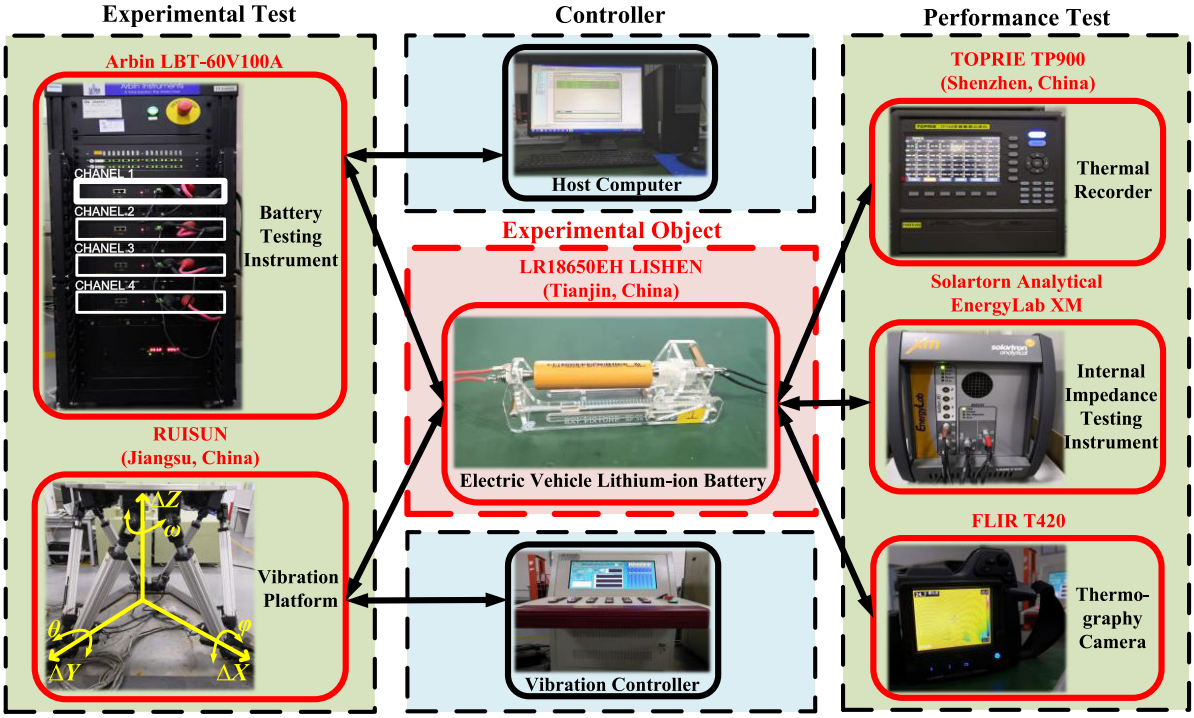

FIGURE 1. The experimental bench under 6-DOF vibration stress and aging stress.

TABLE 2. Characteristics contrast of experimental bench between this paper and others.

Item	Ref. [8]	Ref. [10]	Ref. [17]	Ref. [22]	This Paper
Conduct charging-discharging protocol	×	×	√	√	√
Test internal impedance	×	×	√	√	√
Record thermal measurement	×	×	×	√	√
Reveal thermography	×	×	×	×	√
Provide 6-dof vibration stress	√	×	×	×	√

to certify the initial quality of the tested batteries, these cells were conducted the capacity test and internal resistance test. According to the Ref. [21], [22], the resistance shown in Figure 5 is internal resistance (DC) at 0% SOC after those batteries were conducted three cycles to activate themselves.

B. VIBRATION TEST

In order to simulate the vibration stress of EV, the vibration stress system is shown in Figure 1. The spectrum extracted from real-world road collection in Figure 2 was the input of the vibration stress environment platform. Especially, charging was performed without vibration stress, but discharging was with that [23].

C. AGING TEST

According to [24], [25], this test profile as Figure 3 are applied to the cells.

Charge step: charge at a 1C constant current rate until the cell voltage reached end of charge voltage 3.65V. Then cell was charged at constant voltage of 3.65V while tapering the charge current. Charge was terminated when the charging current has tapered to 0.02C. Rest step: rest for 30min. In order to simulate the driving conditions including four types of speed stages: constant, idle, acceleration and deceleration, discharge step is shown in Figure 3. The cycle lasts about 3.5h.

D. STATIC TEST

As a reference, the cells under this test were not subjected to any stress including vibration stress or aging stress.

The experimental profile is shown in Table 3.

TABLE 3. Experimental profile.

Cell number	#A	#B	#C	#D
Test type	Vibration test with aging test	Aging test	Vibration test	Static test
Test temperature		17.5±0.5 °C		
Test time (cycle)		About 3.5 h		
Test cycles		200 cycles		

IV. TESTS INTRODUCTION

To investigate the varying performance of lithium-ion batteries under different tests, the following tests dependent on the experimental bench introduced in Section 3 were conducted in this paper.

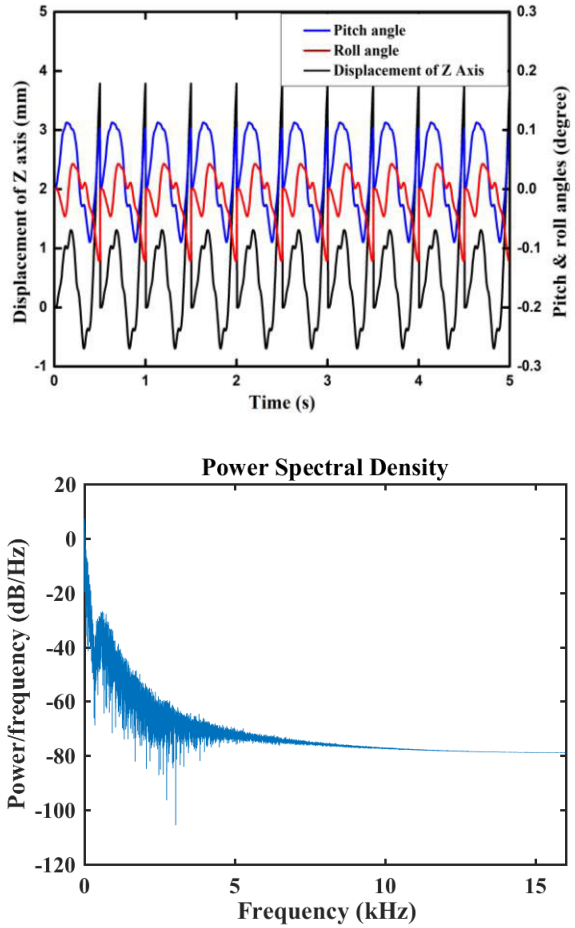

FIGURE 2. The road spectrum and power spectral density of the vibration test.

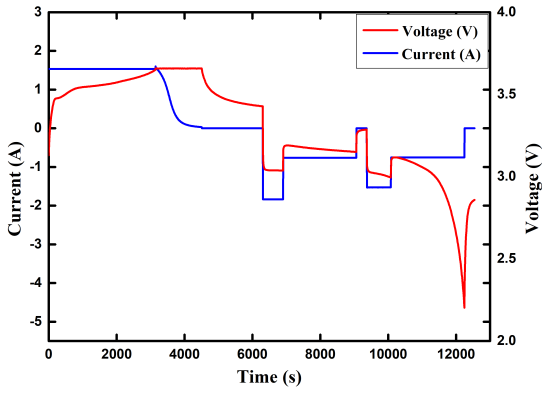

FIGURE 3. The test profile applied to the cells.

A. INTERNAL IMPEDANCE TEST

To investigate the changes on the impedance resistance of cells, the EIS measurement was conducted as rang from 100 kHz to 0.01Hz at AC every ten cycles.

B. OHMIC RESISTANCE TEST

The internal resistance is regarded as one of the crucial parameters for understanding the kinetic characteristics of the cells. And ohmic resistance represents the effects of resistances of the electrodes and electrolyte of the battery. According to the Ref. [21], [22], the ohmic resistance R_o can be extracted from the intersection of the EIS.

C. TEMPERATURE TEST

To reveal the impact of the temperature on cells, this thermal measurement was conducted every ten cycles.

D. CAPACITY TEST

Firstly, the capacity test was under 25 °C. Secondly, the tested batteries were conducted at 0.2C under normal CCCV protocol. The cut-off current at the CV stage is 0.02C. Then, the tested cells were discharged at 0.1C, the cut-off voltage is 2.0V.

V. RESULTS

To reveal the varying performance of lithium-ion batteries under different tests, the tests results in Section 4 are shown as follows.

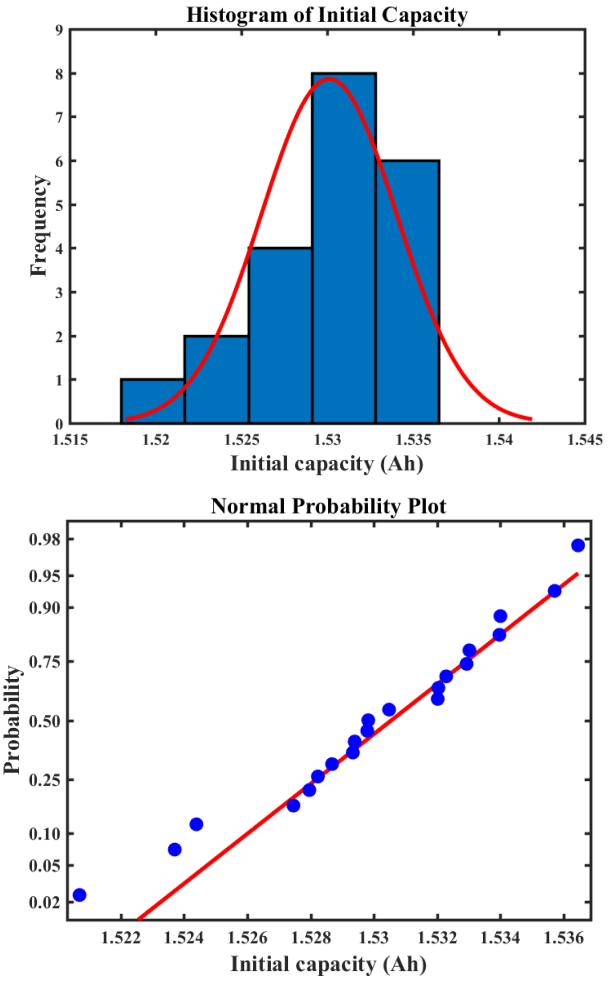

FIGURE 4. Initial characteristics of tested batteries: Initial capacity distribution and normal probability plot of initial capacity distribution.

A. INITIAL CHARACTERISTICS

Figures 4 and 5 show the distribution of the cell initial capacities and resistances that were measured from the

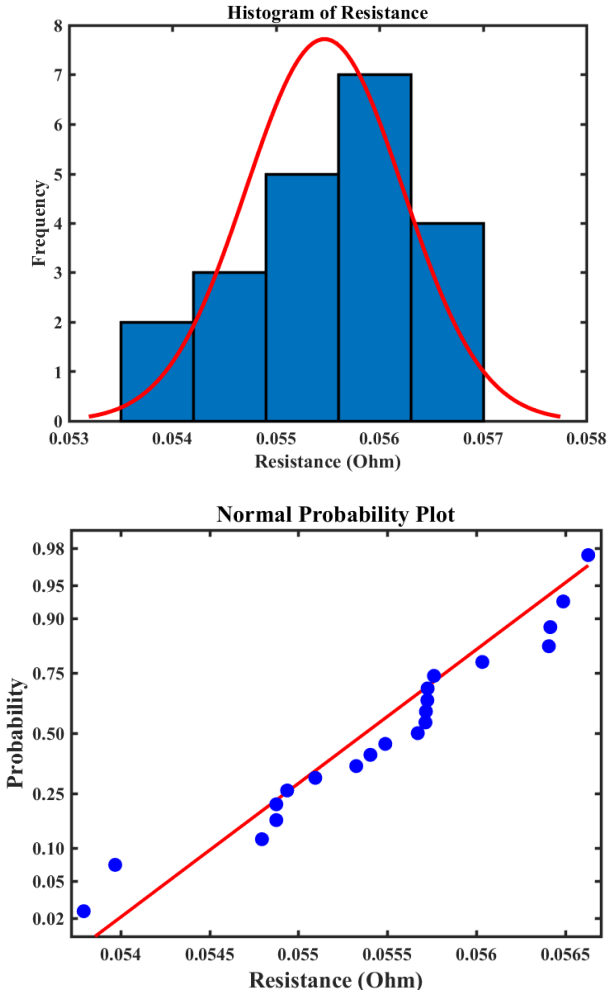

FIGURE 5. Initial characteristics of tested batteries: Resistance distribution and normal probability plot of resistance distribution.

capacity test and the internal resistance test. According to Figure, the capacities of the selected batteries are 1.5301 ± 0.0176 Ah (±1.15%) and the resistances of the batteries are 0.0555 ± 0.0034 Ω (±6.12%). Based on minute variances and the normal distributions of the capacity and resistance, the initial quality of the selected cells was qualified.

B. INTERNAL IMPEDANCE

The intersection of the curve and $\mathrm{Im}\{Z\} = 0$ represents the ohmic impedance (R_o) in the solution that contains the ohmic impedance of the electrode surface to the liquid surface and the activated carbon tunnel on the electrode. R_o is used to evaluate electrolyte degradation, which can be calculated through interpolation of the two neighboring frequency points and below $\mathrm{Im}\{Z\} = 0$.

The inductive behavior is shown in the lower part of the spectrum, which is regard not subject to aging. As for upper part of the spectrum, there are a distorted semicircle and a straight line with slope at the right terminal. This semicircle demonstrates limitations due to the passivation layers and the charge transfer resistances at both electrodes and double layer capacities. This sloping line exhibits the diffusion resistance of the electrolyte ions in the pores of the electrode and the internal contact resistance (the called identifiable Warburg resistance) [26], [27]. Figure 6 displays the Nyquist plot of EIS spectra for the cells under different tests.

#A Cell and #B Cell display more changes than #C Cell and #D Cell between initial and after 200 cycles. In addition, #B Cell shows a smaller slop than #A Cell, and #A Cell exhibits a larger semicircle than #B Cell. Meanwhile, there is no obvious changes in distorted semicircle, however, a bigger semicircle occurs to #A Cell. #C Cell and #D Cell shows the small variances of internal impedances between the vibration test and the static test for 200 cycles. That the changes about kinetic and mass transfer may have taken place can account for these differences between #A Cell and #B Cell.

C. OHMIC RESISTANCES

According to the calculation of the ohmic resistance test, the Figure 7 demonstrates the ohmic resistance R_o of the cells under different experimental profiles (including vibration test with aging test, aging test, vibration test, static test). For the #A Cell and #B Cell (cells under vibration test with aging test, aging test), there is no apparent difference between them at the beginning of the 100 cycles. After 100th cycle, #A Cell shows exhibits a larger growth trend (about 18.8%) and increase of ohmic resistance than #B Cell (about 12.5%). However, for the #C Cell and #D Cell (cells under vibration test and static test), there is no apparent changes at 200 cycles for the ohmic resistance, which concludes that the ohmic resistance of the cells under vibration test and static test may be not subject to vibration stress (without aging stress) [28].

D. THERMAL MEASUREMENT

The thermal failure has an important impact on battery performance. Hence, the impact of vibration stress on thermal feature for cells is revealed as in Figure 8. And thermography of #A Cell and #B Cell at the same moment is displayed in Figure 9. The chemical reactions occurring inside the lithium iron phosphate battery are as follows:

$$LiFePO_4 - xLi^+ - \mathrm{x}e^- \overset{Charge}{\longrightarrow} xFePO_4 + (1-x)\,LiFePO_4 \quad (1)$$

$$FePO_4 + xLi^+ + \mathrm{x}e^- \overset{Discharge}{\longrightarrow} xLiFePO_4 + (1-x)\,LiFePO_4 \quad (2)$$

During the process of discharge, the heat generated inside the battery is mainly composed of this four types of heat: reaction heat, Joule heat, polarization heat and side reaction heat. According to the principle of heat transfer, there are three ways to transfer heat: conduction, convection and radiation. Usually inside the battery, due to the weak flow of the electrolyte, the internal heat convection is negligible. And the heat radiation is also weak. Therefore, the heat that is transferred from the inside of the battery to the case by heat conduction. When exchanging heat with the outside world, the main method is heat convection.

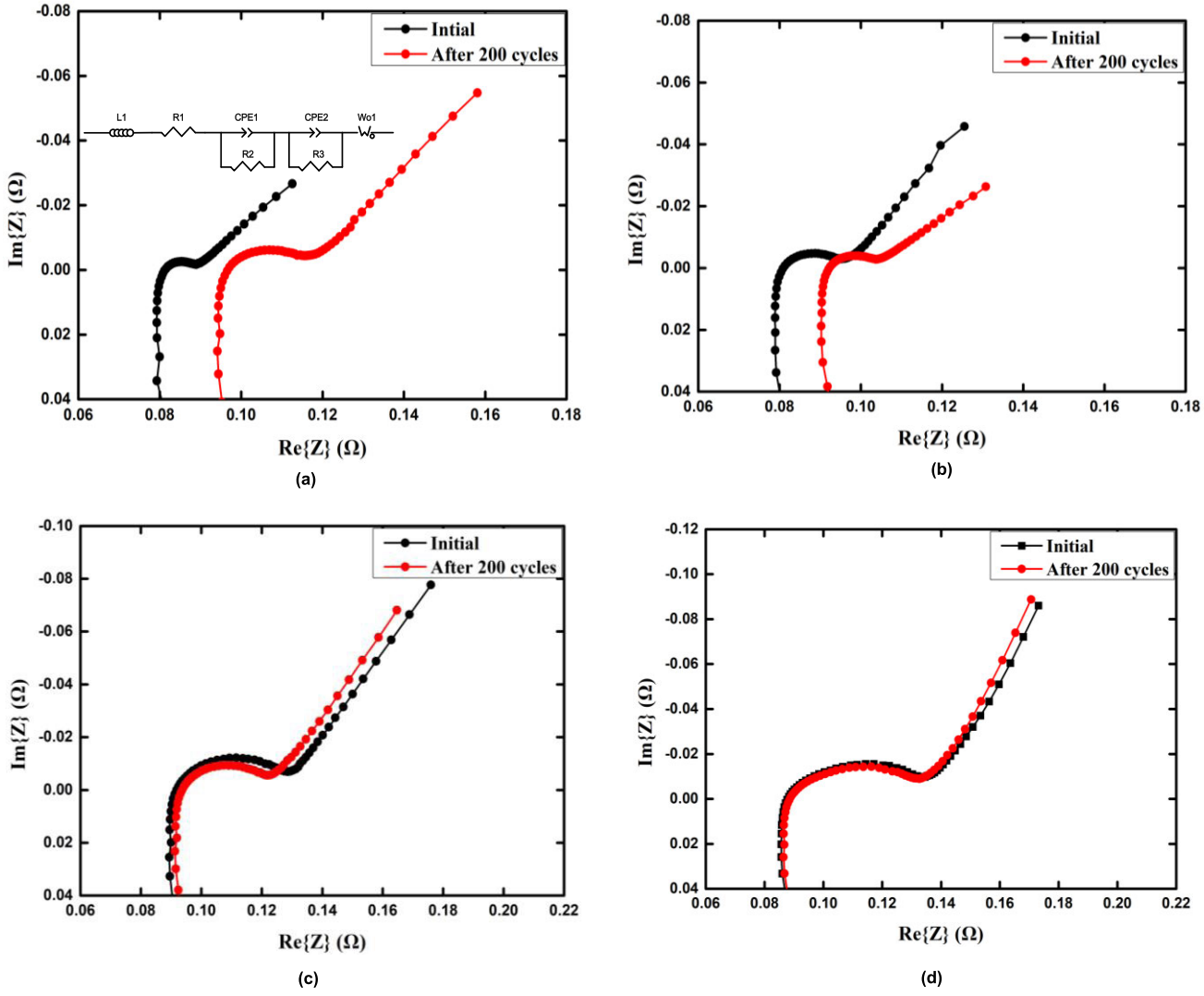

FIGURE 6. Nyquist plot of EIS spectra for cells under different tests: (a) #A Cell under vibration test with test profile and equivalent circuit model of #A Cell. (b) #B Cell under test profile. (c) #C Cell under vibration test. (d) #D Cell under static test.

Figure 8 demonstrates the #A Cell release more heat than #B Cell during the discharging process. Furthermore, the heat of both #A Cell (4°C/200 cycles) and #B Cell (3°C/200 cycles) increases with aging. The maximum difference of the heat is 9.60% and 8.77% for the #A Cell and #B Cell [29]–[32]. Additionally, Figure 9 displays the small variance in the distribution of heat for the cells. According to the principle of heat transfer, the vibration stress may affect the flow of electrolyte inside the battery, resulting in the release of more heat [33]–[35].

E. OCV RECOVERY

OCV is regarded to have close relationship with the natural properties determined by the Gibbs energy in the electrochemical reactions of lithium-ion battery OCV displays the difference between the electrodes' potentials when current is cutoff in the battery. And OCV recovery in this paper is used to describe the phenomenon that terminal voltage changes during the relaxation time. To analyze the impact of vibration stress on OCV recovery, the OCV recovery rate from the beginning and end of the last rest step (about 8 min) was extracted as Figure 10. Owing to aging, the capability of OCV recovery is attenuated, especially #A Cell has a poorer performance on OCV recovery than #B Cell. Other than this, the cutoff voltage of #A Cell is lower than #B Cell during the discharging process, for which #A Cell is considered to have more capacity consumption than #B Cell [36], [37].

Since the OCV of the lithium-ion battery depends on the electrode material and the amount of lithium particulate embedded in the electrode material. For the positive electrode, it refers to the lithium particulate stored in the gaps of the material. When discharge is in process, lithium particulates turn to lithium ions and flow out of the gap. And when the battery is charged, lithium ions are changed back

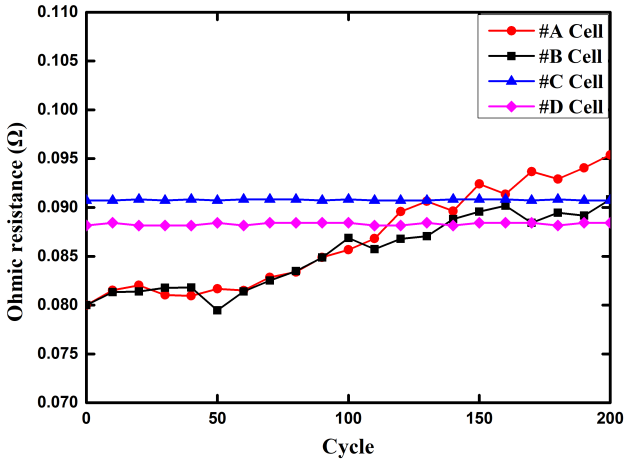

FIGURE 7. The ohmic resistances of the cells under experimental profiles.

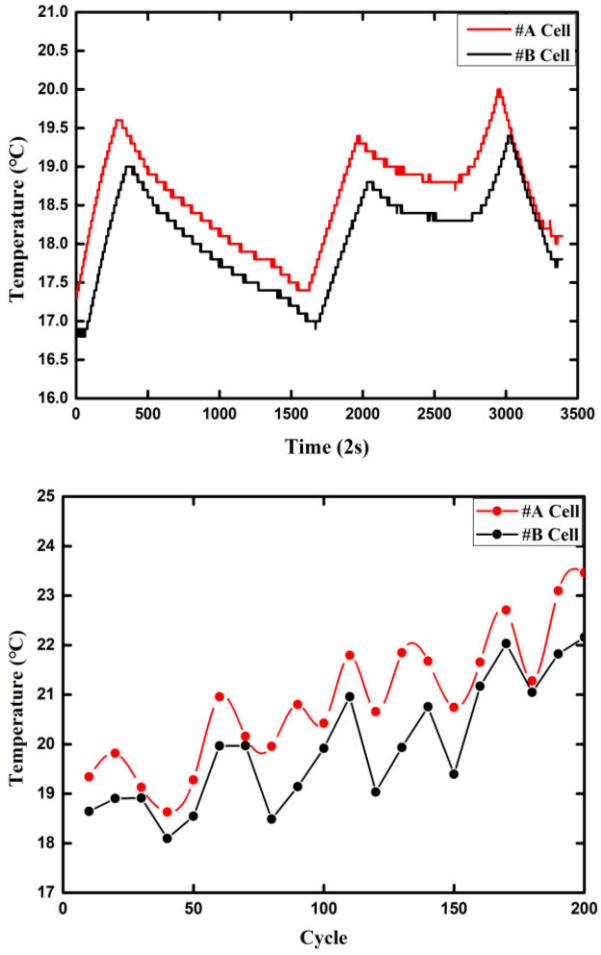

FIGURE 8. Thermal curve during discharge process (up) and average temperature curves of #A Cell and #B Cell (down).

to the lithium particulates and embedded in the gap of the positive electrode material. However, the principle of above process for the negative electrode material is opposite. Hence, it may be concluded that vibration stress have impact on the process of OCV recovery [38], [39].

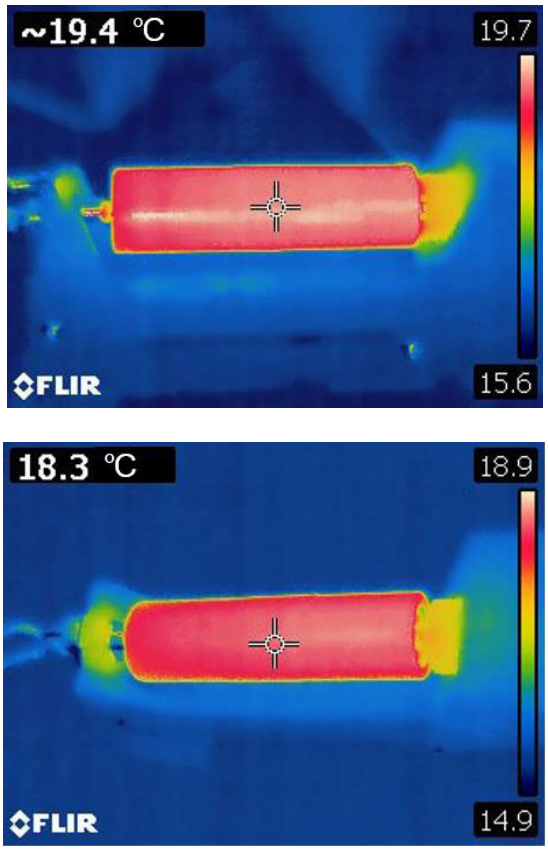

FIGURE 9. Thermography of #A Cell (up) and #B Cell (down) at the same moment.

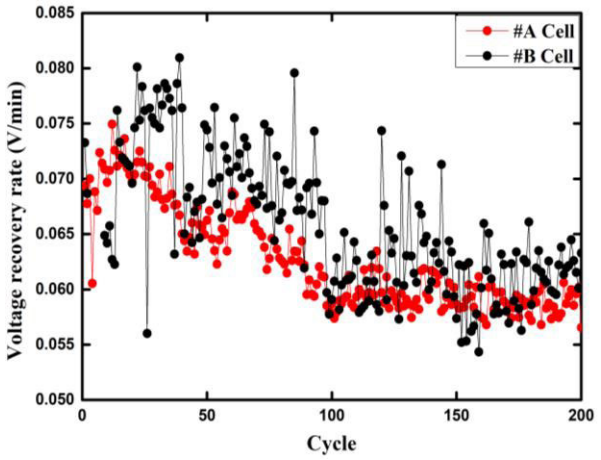

FIGURE 10. OCV recovery rate curve of #A Cell and #B Cell.

F. CAPACITY DEGRADATION

To investigate the effect of vibration stress on cycle life, cells under different tests for 200 cycles were compared, and the results are shown in Figure 11. During the first 80th cycle, the capacity fade of the cells is similar. After that, the capacity fade of #A Cell is faster than #B Cell. The Figure 11 exhibits varying characteristics of the cells under different tests: #A Cell reveals faster degradation (about 0.78 Ah/200 cycles)

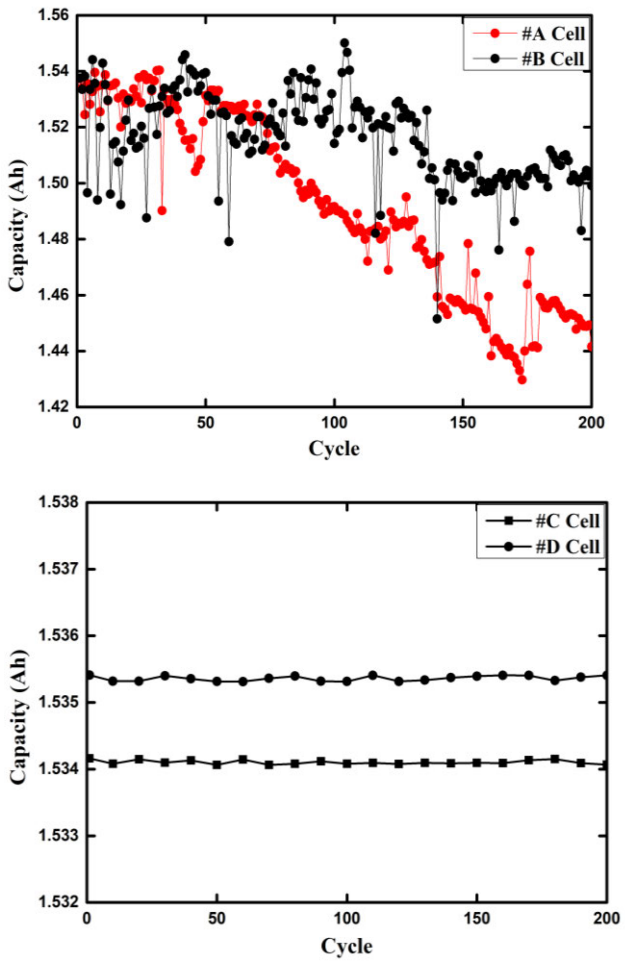

FIGURE 11. The capacity degradation curves of the cells under different tests.

than others (#B Cell: about 0.42 Ah/200 cycles. #C Cell and #D Cell display no obvious fade.), especially after 80th cycle.

Capacity fade is mainly affected by factors as follows [40]–[42]:

1) Changes in the structure of the positive electrode material.

LiFePO4 has an olivine structure and belongs to the orthorhombic crystal, the Pumb space group. The charge-discharge reaction of it is carried out between LiFePO4 and FePO4. The current research shows that the changes in the structure of the positive electrode material LiFePO4 is small during the cycle. Therefore, for the sample of this paper, the main reason for the capacity fade is not the changes in the structure of the positive electrode material.

2) Changes in the structure of the negative electrode material.

There are four forms about the changes in the structure of the negative electrode material: firstly, solvated lithium ion intercalation reaction or solvent co-intercalation reaction, causing damage to the structure of the graphite and resulting in interruption of electronic conductivity. Secondly, formation of solid electrolyte interface (SEI), especially excellent SEI with electronic insulation, passivating graphite. Thirdly, the above two cases occur to battery together, the graphite is passivated, and part of the structure is destroyed.

3) Dissolution of the active substance.

The dissolution of metal elements leads to a decrease in the amount of active substances, which directly affects the capacity loss. Besides, the dissolution of the positive electrode material has impact on the electron transport. What's more, the metal ions in the electrolyte are converted into metal forms, affecting the thickness and stability of the SEI and resulting in an increase in electrode surface polarization. The internal resistance increases finally.

4) Consumption of the lithium ion.

Some of the lithium ions are consumed by SEI, which are irreversible for capacity loss.

5) Increases of the internal resistance.

The oxidation reaction occurs to the electrolyte in the interface of the electrode/electrolyte, leading to an increase in internal resistance of the battery. Moreover, dissolution of metal ions in the positive electrode and formation of metal deposition in the negative electrode are also responsible for an increase in internal resistance.

It is believed that vibration stress may affect some of these above factors, thereby accelerating capacity fade.

VI. STATISTICAL ANALYSIS

The results shown in Section 5 is qualitative analysis, so the ANOVA was used to evaluate the statistical results for the characteristics of the cells to quantify the impact of 6-DOF vibration stress with aging stress.

Section 5 exhibits the cell characteristics in different test, including the internal impedance, internal resistance, thermal measurement, OCV recovery rate and capacity. The characteristics of #A Cell can be compared with the #B Cell to determine the impact of the vibration stress on cells, which is so-called the ANOVA in the statistical field.

The variance of the cell characteristics in different tests ($CC_{different}$) is calculated as Formula (3):

$$CC_{different} = \sum_{i=1}^{r} n_i \left(\overline{x}_i - \overline{x}\right)^2 \tag{3}$$

where n_i is the sample number in group i, $\overline{x}_i$ represents the average of cell characteristics in group i, $\overline{x}$ represents the average of all tested cells characteristics.

The variance of the cell characteristics in the same test (CC_{same}) is calculated as in:

$$CC_{same} = \sum_{i=1}^{5} \sum_{j=1}^{2} \left(\overline{x}_{ij} - \overline{x}_i\right)^2 \tag{4}$$

where $\overline{x}_{ij}$ represents the j cell characteristics in group i, $\overline{x}_i$ represents the average of cell characteristics in group i.

According to the ANOVA, DOF should be taken into consideration. Therefore, mean squares (MS) is defined

TABLE 4. Statistical results for the characteristics of the cells before experiments.

Parameters	F	*P*	Evaluation
Ohmic Resistance	1.89	0.2721	Not Statistically Significant
Polarization Resistance	4.92	0.0788	Not Statistically Significant
Resistance	1.46	0.351	Not Statistically Significant
Thermal Measurement	8.79	0.0975	Not Statistically Significant
Ocv Recovery	0.53	0.5425	Not Statistically Significant
Capacity	3.6	0.1982	Not Statistically Significant

TABLE 5. Statistical results for the characteristics of the cells under the vibration stress with aging stress.

Parameters	F	*P*	Evaluation
Ohmic Resistance	6.47	0.0151	Statistically Significant
Polarization Resistance	0.89	0.351	Not Statistically Significant
Resistance	3.86	0.0567	Not Statistically Significant
Thermal Measurement	5.07	0.0303	Statistically Significant
Ocv Recovery	9.22	0.0025	Statistically Significant
Capacity	7.53	0.0092	Statistically Significant

as follows:

$$MS = \frac{CC}{DOF} \tag{5}$$

And value F of Fisher-test can be calculated as follows:

$$F = \frac{MS_{different}}{MS_{same}} \tag{6}$$

Then p value can be derived from p-value table based on F value and the DOF of the both numerator and denominator in Formula (7). The p value determines whether the vibration stress is ''statistically significant'' to the cell. Generally, the vibration stress is significant when the p value is less than 0.05 [43], [44].

$$P = f\left(F, DOF_{different}, DOF_{same}\right) \tag{7}$$

Table 4 and Table 5 exhibit the statistical results for the characteristics of the cell before experiment and under the 6-DOF vibration stress with aging stress, respectively. Through comparing the statistical results of this two tables, it can be concluded that 6- DOF vibration stress with aging stress has little impact on the cell polarization resistance, while it affects the ohmic resistance, OCV recovery, thermal measurement and capacity of cells, respectively.

VII. CONCLUSION

An experimental test bench, which not only provides 6-DOF vibration stress but also conducts the aging test, was established for analyzing the degradation of lithium-ion battery under external factors. This paper concentrates on the characterization of lithium-ion cells under six-DOF vibration stress considering driving conditions. The cells were conducted four types of tests (vibration test with aging test, aging test, vibration test and static test). The results exhibit that the cells operated under vibration stress show a larger ohmic resistance, a higher release of heat, a lower rate of OCV recovery and a higher rate of capacity degradation than the cells under aging and others. Moreover, the internal impedance of each cell is also changed because of vibration stress.

As for EIS, #A Cell and #B Cell display more changes than #C Cell and #D Cell between initial and after 200 cycles. In addition, #B Cell shows a smaller slop than #A Cell, and #A Cell exhibits a larger semicircle than #B Cell. Meanwhile, there is no obvious changes in distorted semicircle, however, a bigger semicircle occurs to #A Cell. #C Cell and #D Cell shows the small variances of internal impedances between the vibration test and static test for 200 cycles. That the changes about kinetic and mass transfer may have taken place can account for these differences between #A Cell and #B Cell.

The released heat of both #A Cell (4°C/200 cycles) and #B Cell (3°C/200 cycles) increases with aging. Especially, #A Cell reveals faster degradation rate (about 0.78 Ah/200 cycles) than others (#B Cell: about 0.42 Ah/200 cycles. #C Cell and #D Cell display no obvious fade.).

According to analysis of variance (ANOVA), these characteristics were compared statistically to determine the impact of the vibration stress with aging on cells. It can be concluded that vibration stress with aging has little impact on the cell polarization resistance, however, it effects the ohmic resistance, OCV recovery, thermal measurement and capacity of cells, respectively.

In future, the performance characteristics of the batteries under different stress will be concentrated on. And other approaches applied to analysis the characteristics of the batteries would be taken into consideration.

REFERENCES

[1] L. Cai, J. H. Meng, D. I. Stroe, G. Z. Luo, and R. Teodorescu, ''An evolutionary framework for lithium-ion battery state of health estimation,'' *J. Power Sources*, vol. 412, pp. 615–622, Feb. 2019.
[2] M. Sitterly, L. Y. Wang, G. G. Yin, and C. Wang, ''Enhanced identification of battery models for real-time battery management,'' *IEEE Trans. Sustain. Energy*, vol. 2, no. 3, pp. 300–308, Jul. 2011.
[3] J. Meng, G. Luo, and F. Gao, ''Lithium polymer battery state-of-charge estimation based on adaptive unscented Kalman filter and support vector machine,'' *IEEE Trans. Power Electron.*, vol. 31, no. 3, pp. 2226–2238, Mar. 2016.
[4] C.-H. Kim, M.-Y. Kim, and G.-W. Moon, ''A modularized charge equalizer using a battery monitoring ic for series-connected li-ion battery strings in electric vehicles,'' *IEEE Trans. Power Electron.*, vol. 28, no. 8, pp. 3779–3787, Aug. 2013.
[5] N. Shafiei, M. Ordonez, M. Craciun, C. Botting, and M. Edington, ''Burst node elimination in high-power *LLC* resonant battery charger for electric vehicles,'' *IEEE Trans. Power Electron.*, vol. 31, no. 2, pp. 1173–1188, Feb. 2016.
[6] J. Meng, M. Ricco, G. Luo, M. Swierczynski, D.-I. Stroe, A.-I. Stroe, and R. Teodorescu, ''An overview of online implementable SOC estimation methods for lithium-ion batteries,'' *IEEE Trans. Ind. Appl.*, vol. 54, no. 2, pp. 1583–1591, Mar./Apr. 2018.
[7] *IEEE Draft Recommended Practice for Stationary Battery Electrolyte Spill Containment and Management*, IEEE Standard P1578/D2, Jun. 2017.
[8] J. Hooper, J. Marco, G. H. Chouchelamane, J. S. Chevalier, and D. Williams, ''Multi-axis vibration durability testing of lithium ion 18650 NCA cylindrical cells,'' *J. Energy Storage*, vol. 15, pp. 103–123, Feb. 2018.
[9] C. Zhang, F. Dang, Y. Chen, Y. Yan, Y. Liu, and X. Chen, ''Vibration-to-electric energy conversion with porous graphene oxide-nickel electrode,'' *J. Power Sources*, vol. 368, pp. 73–77, Nov. 2017.

[10] M. J. Brand, S. F. Schuster, T. Bach, E. Fleder, M. Stelz, S. Gläser, J. Müller, G. Sextl, and A. Jossen, "Effects of vibrations and shocks on lithium-ion cells," *J. Power Sources*, vol. 288, pp. 62–69, Aug. 2015.

[11] J. Meng, D. Stroe, M. Ricco, G. Luo, M. Swierczynski, and R. Teodorescu, "A novel multiple correction approach for fast open circuit voltage prediction of lithium-ion battery," *IEEE Trans. Energy Conver.*, vol. 34, no. 2, pp. 1115–1123, Jun. 2019.

[12] A. H. Hosseinloo and M. M. Ehteshami, "Shock and vibration effects on performance reliability and mechanical integrity of proton exchange membrane fuel cells: A critical review and discussion," *J. Power Sources*, vol. 364, pp. 367–373, Oct. 2017.

[13] S.-K. Hong, B. I. Epureanu, and M. P. Castanier, "Parametric reduced-order models of battery pack vibration including structural variation and prestress effects," *J. Power Sources*, vol. 261, pp. 101–111, Sep. 2014.

[14] K.-Y. Oh and B. I. Epureanu, "A phenomenological force model of li-ion battery packs for enhanced performance and health management," *J. Power Sources*, vol. 365, pp. 220–229, Oct. 2017.

[15] P. J. Swornowski, "Destruction mechanism of the internal structure in lithium-ion batteries used in aviation industry," *Energy*, vol. 122, pp. 779–786, Mar. 2017.

[16] A. A. A. Al-Karakchi, G. Lacey, and G. Putrus, "A method of electric vehicle charging to improve battery life," in *Proc. 50th Int. Univ. Power Eng. Conf. (UPEC)*, Stoke on Trent, U.K., 2015, pp. 1–3.

[17] P. Keil and A. Jossen, "Charging protocols for lithium-ion batteries and their impact on cycle life—An experimental study with different 18650 high-power cells," *J. Energy Storage*, vol. 6, pp. 14–125, May 2016.

[18] X. Hu, H. Yuan, C. Zou, Z. Li, and L. Zhang, "Co-estimation of state of charge and state of health for lithium-ion batteries based on fractional-order calculus," *IEEE Trans. Veh. Technol.*, vol. 67, no. 11, pp. 10319–10329, Nov. 2018.

[19] W. Li, Z. Jiao, L. Du, W. Fan, and Y. Zhu, "An indirect RUL prognosis for lithium-ion battery under vibration stress using Elman neural network," *Int. J. Hydrogen Energy*, vol. 44, no. 23, pp. 12270–12276, Apr. 2019.

[20] W. Li, Z. Jiao, and L. Zhou, "Analysis of performance degradation and residual life prediction of batteries for electric vehicles under driving conditions," *IEEJ Trans. Elect. Electron. Eng.*, vol. 14, no. 3, pp. 493–498, Mar. 2019.

[21] M. Galeotti, L. Cinà, C. Giammanco, S. Cordiner, and A. Di Carloac, "Performance analysis and SOH (state of health) evaluation of lithium polymer batteries through electrochemical impedance spectroscopy," *Energy*, vol. 89, pp. 678–686, Sep. 2015.

[22] L. Su, J. Zhang, H. Ge, Z. Li, F. Xie, and B. Y. Liaw, "Path dependence of lithium ion cells aging under storage conditions," *J. Power Sources*, vol. 315, pp. 35–46, May 2016.

[23] B. He, H. Wang, and X. He, "Vibration test methods and their experimental research on the performance of the lead-acid battery," *J. Power Sources*, vol. 268, pp. 326–330, Dec. 2014.

[24] M. Ecker, J. B. Gerschler, J. Vogel, S. Käbitz, F. Hust, P. Dechent, and D. U. Sauer, "Development of a lifetime prediction model for lithium-ion batteries based on extended accelerated aging test data," *J. Power Sources*, vol. 215, pp. 248–257, Oct. 2012.

[25] J.-H. Ahn and B. K. Lee, "High-efficiency adaptive-current charging strategy for electric vehicles considering variation of internal resistance of lithium-ion battery," *IEEE Trans. Power Electron.*, vol. 34, no. 4, pp. 3041–3052, Apr. 2019.

[26] X. Hu, S. E. Li, and Y. Yang, "Advanced machine learning approach for lithium-ion battery state estimation in electric vehicles," *IEEE Trans. Transport. Electrific.*, vol. 2, no. 2, pp. 140–149, Jun. 2016.

[27] B. G. Carkhuff, P. A. Demirev, and R. Srinivasan, "Impedance-based battery management system for safety monitoring of lithium-ion batteries," *IEEE Trans. Ind. Electron.*, vol. 65, no. 8, pp. 6497–6504, Aug. 2018.

[28] M. I. Wahyuddin, P. S. Priambodo, and H. Sudibyo, "Direct current load effects on series battery internal resistance," in *Proc. 15th Int. Conf. Qual. Res. (QiR), Int. Symp. Elect. Comput. Eng.*, Nusa Dua, Indonesia, 2017, pp. 120–123.

[29] X. Tang, Y. Wang, C. Zou, K. Yao, Y. Xia, and F. Gao, "A novel framework for lithium-ion battery modeling considering uncertainties of temperature and aging," *Energy Convers. Manage.*, vol. 180, pp. 162–170, Jan. 2019.

[30] W. Wu, S. Wang, W. Wu, K. Chen, S. Hong, and Y. Lai, "A critical review of battery thermal performance and liquid based battery thermal management," *Energy Convers. Manage.*, vol. 182, pp. 262–281, Feb. 2019.

[31] Y. Cao, R. C. Kroeze, and P. T. Krein, "Multi-timescale parametric electrical battery model for use in dynamic electric vehicle simulations," *IEEE Trans. Transport. Electrific.*, vol. 2, no. 4, pp. 432–442, Dec. 2016.

[32] W. Renhart, C. Magele, and B. Schweighofer, "FEM-based thermal analysis of NiMH batteries for hybrid vehicles," *IEEE Trans. Magn.*, vol. 44, no. 6, pp. 802–805, Jun. 2008.

[33] M. G. Jeong, J.-H. Cho, and B. J. Lee, "Heat transfer analysis of a high-power and large-capacity thermal battery and investigation of effective thermal model," *J. Power Sources*, vol. 424, pp. 35–41, Jun. 2019.

[34] A. Börger, J. Mertens, and H. Wenzl, "Thermal runaway and thermal runaway propagation in batteries: What do we talk about?" *J. Energy Storage*, vol. 24, Aug. 2019, Art. no. 100649.

[35] J. Zhang, L. Zhang, F. Sun, and Z. Wang, "An overview on thermal safety issues of lithium-ion batteries for electric vehicle application," *IEEE Access*, vol. 6, pp. 23848–23863, May 2018.

[36] T. Gallien, H. Krenn, R. Fischer, S. Lauterbach, B. Schweighofer, and H. Wegleiter, "Magnetism versus $LiFePO_4$ battery's state of charge: A feasibility study for magnetic-based charge monitoring," *IEEE Trans. Instrum. Meas.*, vol. 64, no. 11, pp. 2959–2964, Nov. 2015.

[37] C. Wu, C. Ke, C. Chang, and Z. Chiou, "Useful life characteristics of a $LiFePO_4$ battery for estimating state of battery health," in *Proc. IEEE Int. Conf. Appl. Syst. Invention (ICASI)*, Chiba, Japan, Apr. 2018, pp. 1338–1341.

[38] M. Petzl and M. A. Danzer, "Advancements in OCV measurement and analysis for lithium-ion batteries," *IEEE Trans. Energy Convers.*, vol. 28, no. 3, pp. 675–681, Sep. 2013.

[39] L. Lavigne, J. Sabatier, J. M. Francisco, F. Guillemard, and A. Noury, "Lithium-ion open circuit voltage (OCV) curve modelling and its ageing adjustment," *J. Power Sources*, vol. 324, pp. 694–703, Aug. 2016.

[40] X. Li, Q. Wang, Y. Yang, and J. Kang, "Correlation between capacity loss and measurable parameters of lithium-ion batteries," *Appl. Energy*, vol. 110, pp. 819–826, Sep. 2019.

[41] M. Dubarry and B. Y. Liaw, "Identify capacity fading mechanism in a commercial $LiFePO_4$ cell," *J. Power Sources*, vol. 194, no. 1, pp. 541–549, Oct. 2009.

[42] S.-H. Wu and P.-H. Lee, "Storage fading of a commercial 18650 cell comprised with NMC/LMO cathode and graphite anode," *J. Power Sources*, vol. 349, pp. 27–36, May 2017.

[43] S. Kim and J. Park, "Hybrid feature selection method based on neural networks and cross-validation for liver cancer with microarray," *IEEE Access*, vol. 6, pp. 78214–78224, 2018.

[44] S. Vergura, G. Acciani, V. Amoruso, G. E. Patrono, and F. Vacca, "Descriptive and inferential statistics for supervising and monitoring the operation of PV plants," *IEEE Trans. Ind. Electron.*, vol. 56, no. 11, pp. 4456–4464, Nov. 2009.

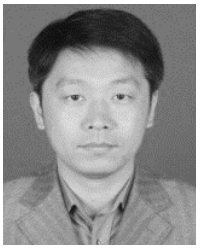

WENHUA LI (M'16) received the Ph.D. degree in electrical engineering from the Hebei University of Technology, in 2006.

He is currently a Professor with the Hebei University of Technology. He has authored one book, more than 50 articles, more than 11 inventions, and 7 software copyrights. His research field includes the analysis of the reliability and detection technology of electrical appliance and new energy and smart gird technology.

Dr. Li was a recipient of the National Science and Technology Prize, a provincial- and ministerial-level science and technology prize (China). He has guided his students to get a Second Prize of the 2016 Certificate Authority Cup International Mathematical Contest in Modeling.

ZHIPENG JIAO received the B.S. degree from the School of Artificial Intelligence, Hebei University of Technology, Tianjin, China, in 2017, where he is currently pursuing the M.S. degree in electrical engineering.

His research interest includes performance analysis and remaining useful life prognosis for lithium-ion battery.

QIAN XIAO received the B.S. and M.S. degrees in electrical engineering from the Hebei University of Technology, Tianjin, China, in 2011 and 2014, respectively. He is currently pursuing the Ph.D. degree in electrical engineering with Tianjin University, Tianjin.

Since November 2018, he has been a Visiting Researcher with the Department of Energy Technology, Aalborg University, Aalborg, Denmark. His research interests include multilevel converters, dc/dc converters, power electronics for distributed generation, microgrid, and HVDC.

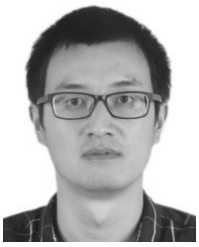

JINHAO MENG (S'14) received the M.S. degree in control theory and control engineering and the Ph.D. degree in electrical engineering from Northwestern Polytechnical University (NPU), Xi'an, China, in 2013 and 2019, respectively. He was supported by the China Scholarship Council as a joint Ph.D. Student with the Department of Energy Technology, Aalborg University, Aalborg, Denmark, from 2017 to 2018.

His research interests include battery modeling, battery states estimation, and energy management.

YUNFEI MU (M'11) was born in Hebei, China. He received the Ph.D. degree from the School of Electrical Engineering and Automation, Tianjin University, Tianjin, China, in 2012, where he is currently an Associate Professor. His research interests include integrated energy systems, electric vehicles, and smart grids.

HONGJIE JIA received the Ph.D. degree in electrical engineering from Tianjin University, China, in 2001.

He became an Associate Professor with Tianjin University, in 2002, and was promoted to Professor, in 2006. His research interests include power reliability assessment, stability analysis and control, distribution network planning and automation, and smart grids.

REMUS TEODORESCU (S'94–M'99–SM'02–F'12) received the Dipl.Ing. degree in electrical engineering from the Polytechnical University of Bucharest, Bucharest, Romania, and the Ph.D. degree in power electronics from the University of Galati, Galati, Romania, in 1989 and 1994, respectively.

In 1998, he joined the Department of Energy Technology, Power Electronics Section, Aalborg University, Aalborg, Denmark, where he is currently a Professor. He was the Coordinator of the Vestas Power Program, from 2007 to 2013, where he was involved in ten Ph.D. projects in the areas of power electronics, power systems, and energy storage. He has published over 200 papers and one book entitled *Grid Converters for Photovoltaic and Wind Power Systems* (Wiley, 2011). He holds six patents. His current research interests include modular multilevel converter, HV silicon-carbide devices, design and control of power converters used in wind power systems, photovoltaics and high-voltage dc transmission/flexible ac transmission systems, and energy storage systems based on Li batteries.

Dr. Teodorescu was an Associate Editor of the IEEE TRANSACTIONS ON POWER ELECTRONICS and the Chair of the IEEE Danish Joint IEEE Industrial Electronics Society, the IEEE Power Electronics Society, and the IEEE Industry Applications Society Chapter.

FREDE BLAABJERG (S'86–M'88–SM'97–F'03) received the Ph.D. degree in electrical engineering from Aalborg University, in 1995, and the honoris causa degree from University Politehnica Timisoara (UPT), Romania, and Tallinn Technical University (TTU), Estonia.

He was with ABB-Scandia, Randers, Denmark, from 1987 to 1988. He became an Assistant Professor, in 1992, an Associate Professor, in 1996, and a Full Professor of power electronics and drives, in 1998, with Aalborg University, where he has been a Villum Investigator, since 2017. He has published more than 600 journal papers in the fields of power electronics and its applications. He has coauthored four monographs and is an Editor of ten books in power electronics and its applications. His current research interests include power electronics and its applications, such as wind turbines, PV systems, reliability, harmonics, and adjustable speed drives.

Dr. Blaabjerg has received 30 IEEE Prize Paper Awards, the IEEE PELS Distinguished Service Award, in 2009, the EPE-PEMC Council Award, in 2010, the IEEE William E. Newell Power Electronics Award, in 2014, the Villum Kann Rasmussen Research Award, in 2014, and the Global Energy Prize, in 2019. He was the Editor-in-Chief of the IEEE TRANSACTIONS ON POWER ELECTRONICS, from 2006 to 2012. He has been a Distinguished Lecturer of the IEEE Power Electronics Society, from 2005 to 2007, and the IEEE Industry Applications Society, from 2010 to 2011 and 2017 to 2018. From 2019 to 2020, he serves as the President of the IEEE Power Electronics Society. He is the Vice-President of the Danish Academy of Technical Sciences too. He was nominated by Thomson Reuters to be between the most 250 cited researchers in Engineering in the world, from 2014 to 2018.